



ELSEVIER

Contents lists available at SciVerse ScienceDirect

Physica B

journal homepage: www.elsevier.com/locate/physb

Size dependent electron momentum density distribution in ZnS

M.C. Mishra^{a,b}, R. Kumar^b, G. Sharma^{c,*}, Y.K. Vijay^b, B.K. Sharma^b^a Department of Physics, Government College Jhunjhunu, Jhunjhunu 303001, India^b Department of Physics, University of Rajasthan, Jaipur 302004, India^c Department of Physics, Banasthali University, Banasthali 304022, India

ARTICLE INFO

Article history:

Received 23 June 2011

Received in revised form

16 August 2011

Accepted 24 August 2011

Available online 26 August 2011

Keywords:

X-ray scattering

Electron momentum density

Ionic model

Charge transfer

ABSTRACT

In this paper, we present size dependent electron momentum density distribution in ZnS. ZnS nanoparticles of size 3.8 nm and 2.4 nm are synthesized using the chemical route and characterized by X-ray diffraction (XRD). The Compton profile measurements are performed on both the nano-sized as well as bulk ZnS samples employing 59.54 keV gamma-rays from ²⁴¹Am source. The results reveal that the valence electron density in momentum space becomes narrower with reduction of particle size. To evaluate the charge transfer on compound formation, the ionic model based calculations for a number of configurations of Zn^{+x}S^{-x} (0.0 ≤ x ≤ 2) are also performed utilizing free atom Compton profiles. These results suggest different amounts of charge transfer in these materials varying from 1.2 to 2.0 electron from Zn to S atom.

© 2011 Elsevier B.V. All rights reserved.

1. Introduction

In the last two decades, materials with reduced dimensions have attracted significant attention and growing interest due to their unique electronic, optical and magnetic properties, which are different from their bulk counterparts [1,2]. Among these, II–VI group semiconductor materials are most attractive because of their technological applications [3–8]. ZnS is an important member of this family and hence has been extensively studied. It is widely used as an important phosphor for photoluminescence (PL) [9], electroluminescence (EL) [10] devices and is also a very attractive material in optical applications especially in nanocrystalline form [11,12]. It has a wide optical band gap 3.6 eV [13] and has two different crystal structures (zinc blende and wurtzite), both of which exhibit direct band gap [14,15].

Regarding nanocrystalline ZnS, a number of investigations have been performed to explore the electronic, structural and optical properties [16–21]. Saravanan et al. [16] synthesized the ZnS nanoparticles using the sol–gel method and characterized them by XRD and SEM probes. They have also analyzed the bonding feature of ZnS nanoparticles using the maximum entropy method and found 0.433 e/Å³ electron density at the middle of the bond between Zn and S atom. The variation of admittance with frequency on the CdS and ZnS quantum dots has been reported by Nath et al. [17], and these results indicated their potential application in electronics as nano-tuned and nano-highpass filters. Zhang et al. [18] have studied the structural character, energetics and electronic properties of

ZnS nanostructures by employing first-principles calculations based on generalized gradient approximation (GGA). They observed that ZnS nanoclusters have stronger quantum confinement effects than ZnS nanotubes. Zhang et al. [19] also reported the size dependent structural and electronic properties of ZnS using first-principles calculations. Navaneethan et al. [20] reported the temperature dependence of morphology, structural and optical properties of ZnS nanostructures. They observed that the absorption edge of the nanoparticles (295 nm) was shifted towards shorter wavelength compared to bulk ZnS due to the quantum confinement effect. Pressure-induced structural transitions of the ZnS nano-particles with different sizes were investigated by Pan et al. [21] by energy dispersive X-ray diffraction (EDXD) from ambient pressure to 35.0 GPa. They found that ZnS nano-particles initially in the zinc blende phase transformed to cubic NaCl structure in the presence of pressure and the transition was reversible when the pressure was released. Thus, it is possible to tune the electronic, structural and optical properties of ZnS nanoparticles by varying their size, making them promising materials for numerous applications.

It is well known that electron momentum density (EMD) is also one of the important ground state property. In the last few decades, measurement of Compton profile has become a powerful tool for the determination of EMDs. It arises due to the fact that within impulse approximation, the measured double differential cross section for inelastically scattered photons is directly related to Compton profile, $J(p_z)$ [22,23],

$$\frac{d^2\sigma}{d\Omega d\omega_2} = C(\omega_1, \omega_2, p_z, \phi) J(p_z) \quad (1)$$

where ω_1 and ω_2 are the energies of photons before and after scattering, respectively. The quantity $C(\omega_1, \omega_2, p_z, \phi)$ depends on

* Corresponding author. Tel.: +91 1438228648; fax: +91 1438228649.
E-mail address: gsphysics@gmail.com (G. Sharma).

the experimental setup while p_z is the electron momentum along the scattering vector (z -axis) and $d\Omega$ is the elemental solid angle. The Compton profile, $J(p_z)$, is related to EMD through the relation

$$J(p_z) = \int_{-\infty}^{+\infty} \int_{-\infty}^{+\infty} \rho(p_x, p_y, p_z) dp_x dp_y \quad (2)$$

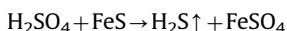
where $\rho(p_x, p_y, p_z)$ is the EMD and the p_z axis is parallel to the photon scattering vector [22,23]. Since, valence electron density is delocalized in r -space, the corresponding quantity in momentum space i.e. valence electron momentum density is localized. This produces narrow contribution in the Compton profile, $J(p_z)$. For this reason, the Compton scattering technique is considered as a promising tool to investigate the behavior of valence electrons.

Although, bulk ZnS has been studied by this technique earlier [24], to our knowledge there is no reported measurement on nano-sized ZnS. In this paper, we report the first-ever size dependent EMD distribution in ZnS. There are no rigorous theoretical prescriptions for computation of Compton profiles for nano-ZnS. Hence, the present experimental data is compared with the corresponding data of bulk sample and also with the free atom theoretical profile to see the effect of particle size on the EMD distribution. Accordingly, a new measurement on bulk ZnS has also been done under identical experimental conditions. In order to examine the difference in the amount of charge transfer in nano-samples relative to bulk ZnS, the ionic model based calculations have also been performed utilizing the free atom Compton profiles of Zn and S [25]. The paper is organized as follows: Section 2 gives details of the experiment. In Section 3, the results and discussions are given. The conclusions are drawn in Section 4. In this paper, unless stated, all quantities are in atomic units (a.u.) where $e = \hbar = m = 1$ and $c = 137.036$, giving unit momentum = $1.9929 \times 10^{-24} \text{ kg m s}^{-1}$, unit energy = 27.212 eV and unit length = $5.2918 \times 10^{-11} \text{ m}$.

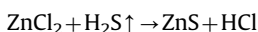
2. Experiment

2.1. Synthesis of nanoparticles

The aqueous solution of 0.01 M of zinc chloride (ZnCl_2) was prepared in de-ionized water using magnetic stirrer for 3 h. Mercaptoethanol was added to zinc chloride solution used as a capping agent at different molar concentrations ranging from 0.005 M to 0.025 M. Hydrogen sulfide gas was produced by following chemical reaction of iron sulfide and sulfuric acid (H_2SO_4) acid:



By the following reaction,



this mixture with H_2S gas at room temperature turned into milky color. The precipitate was filtered and washed 3–4 times with distilled water. Finally the precipitate was dried in vacuum for 24 h to obtain fine ZnS nanomaterial.

2.2. Compton profile measurements

The ^{241}Am gamma-ray spectrometer described by Sharma et al. [26] has been employed for the Compton profile measurements. The incident gamma rays of 59.54 keV from 5 Ci annular ^{241}Am source were scattered at an angle $166^\circ \pm 3.0^\circ$ by the bulk and nanocrystalline samples of ZnS. The details regarding samples, measurement time and number of counts collected are given in Table 1. The scattering chamber was evacuated to about 10^{-2} Torr with a rotary oil pump to reduce the contribution of air scattering and the samples were held vertical by affixing on the back of the lead covered brass slab with a hole of radius 9.05 mm. The scattered radiation was analyzed using an HPGe detector (Canberra model, GL0110S), which was cooled with liquid nitrogen providing overall momentum resolution 0.6 a.u. The spectra were recorded with a multichannel analyzer (MCA) with 4096 channels. The channel width was $\sim 20 \text{ eV}$, corresponding to 0.03 a.u. of momentum. To correct for the background, measurement with empty sample holder was performed for 24 h and the measured background was subtracted from the raw data channel by channel after scaling it to the actual counting time. Thereafter, the corrected background spectra were processed for several corrections like instrumental resolution, sample absorption and scattering cross section using computer code of the Warwick group [27,28] to obtain the Compton profiles. After converting the profiles to the momentum scale, a Monte Carlo simulation was performed to account for the multiple scattering corrections in the samples. To account for multiple scattering corrections history of approximately 10^7 photons were considered. The effect of multiple scattering was found to be 4.70%, 2.9% and 2.1% in the range -10 a.u. to $+10 \text{ a.u.}$ for bulk, samples A and B of nano-ZnS, respectively. Finally, the corrected profiles were normalized to 20.24 electrons in the range 0 a.u. to $+7 \text{ a.u.}$, being the area of free atom Compton profile [25] in the given range. In the present experimental setup, the K electrons of Zn contribute up to 2.2 a.u. only.

3. Results and discussion

The phase purity and crystal structure of these samples were analyzed using a Philips X'pert Pro X-Ray diffractometer having $\text{Cu K}\alpha$ ($\lambda = 1.5460 \text{ \AA}$) source of X-rays. The three main diffraction peaks indexed at (1 1 1), (2 2 0) and (3 1 1) were observed near 2θ angles of 28.50° , 47.66° and 56.54° , respectively, are shown in Fig. 1. Comparison of recorded XRD pattern with standard JCPDS 80.0020 data file confirms the zinc blende (cubic) structure of nanocrystalline samples of ZnS (nano-A and nano-B). The average particle size of ZnS nanoparticles was calculated from the broadening of diffraction peaks using the Debye–Scherrer formula [29]. The particle size obtained from XRD pattern is 3.8 nm and 2.4 nm for samples A and B, respectively, and it is confirmed that particle size decreased with increasing capping agent concentration.

The size and morphologies of the synthesized ZnS nanoparticles were examined using scanning electron microscopy (SEM)

Table 1
Some details concerning the samples and measurements.

| Sample ZnS | Sample thickness (mm) | Density (gm/cm^3) ^a | Counts at Compton peak ($\times 10^4$) | Multiple scattering (-10 to $+10 \text{ a.u.}$) % | Exposure time (h) | Normalization (0 to $+7 \text{ a.u.}$) e^- |
|------------|-----------------------|---|--|---|-------------------|---|
| Bulk | 0.32 | 1.3606 | 2.75 | 4.79 | 25 | 20.24 |
| Nano-A | 0.32 | 0.6795 | 2.60 | 2.9 | 26 | 20.24 |
| Nano-B | 0.32 | 0.4995 | 2.10 | 2.1 | 25 | 20.24 |

^a Effective density of the sample.

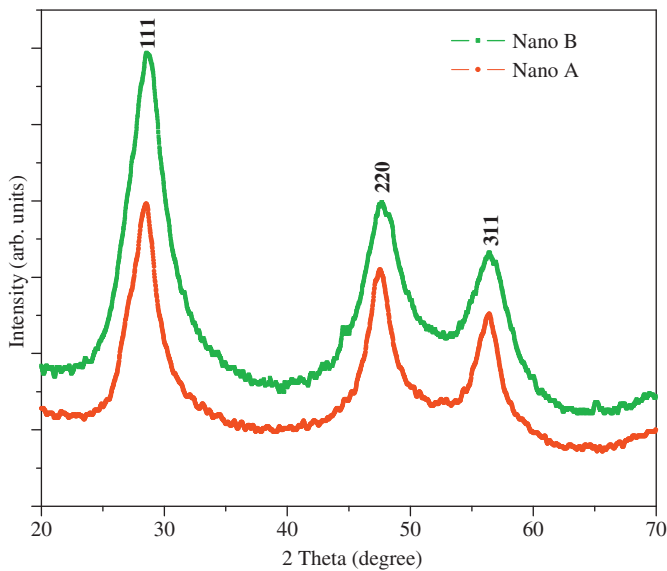


Fig. 1. XRD patterns of ZnS nanoparticles of different sizes.

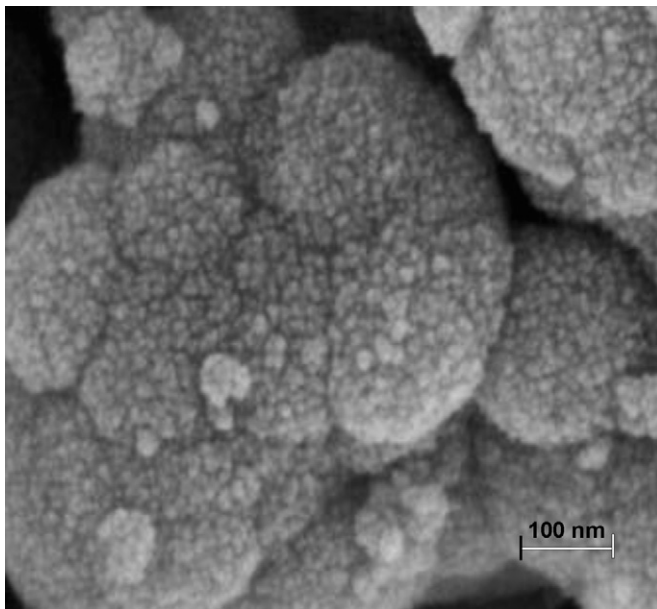


Fig. 2. SEM image of ZnS nanocrystalline sample (nano-A).

and transmission electron microscopy (TEM). Fig. 2 represents image of ZnS nanoparticles obtained from high resolution SEM at highest magnification for nano-A sample. The scanning electron microscopy allows imaging of individual crystallites and the development of a statistical description of the size and shape of the particles in a sample. It highlights the presence of spherical, monodisperse and uniformly distributed nanoparticles. The particles as seen in the SEM pictures are nanoaggregates of many nanoparticles and individual crystallite size is expected to be much less. The actual size of nanoparticles cannot be determined from SEM. The figure shows that the particle size distribution is less than 100 nm in diameter for nano-A sample. The discrepancy with size of ZnS nanoparticles may be because of the fact that SEM shows the lateral dimension of the particles whereas XRD gives the regularity in the atomic arrangement.

The TEM is often used to deduce a mean particle size and size distributions from a limited number of particle images.

A representative TEM image of ZnS (nano-A) is displayed in Fig. 3. The mean size of these nanoparticles from TEM observation is about 5–7 nm. In the TEM image, lattice fringes can be clearly observed, which indicate that the particles are crystalline. However, the particles were not aggregated into a big structure, although particles were in contact with each other. Most of the particles were similar in size and had irregular rounded shapes.

In Fig. 4, the present experimental data on bulk ZnS (obtained from 59.54 keV gamma-rays) is compared with the earlier published data [24]. It is clearly visible that the agreement between two data is very good and beyond 2.0 a.u. The inset shows the difference curve shown in the inset points out the subtle differences in low momentum region, which may perhaps be due to the differences in data correction procedure in the experiments, specially deconvolution and multiple scattering corrections.

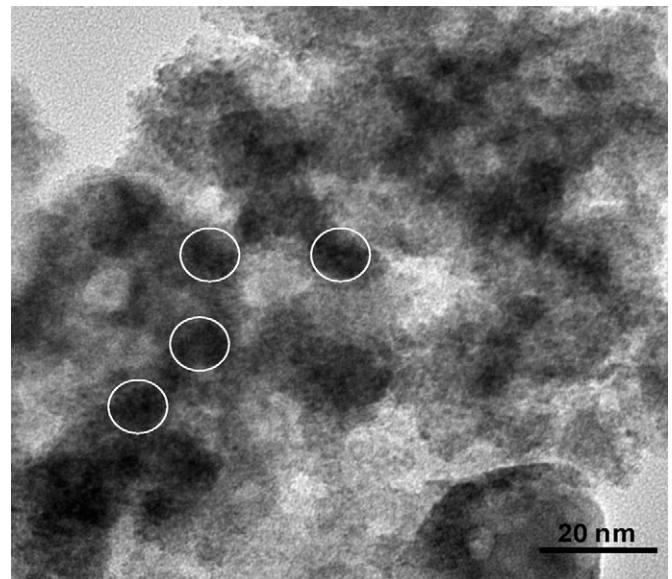


Fig. 3. Transmission electron microscopy (TEM) image of ZnS nanocrystalline sample (nano-A).

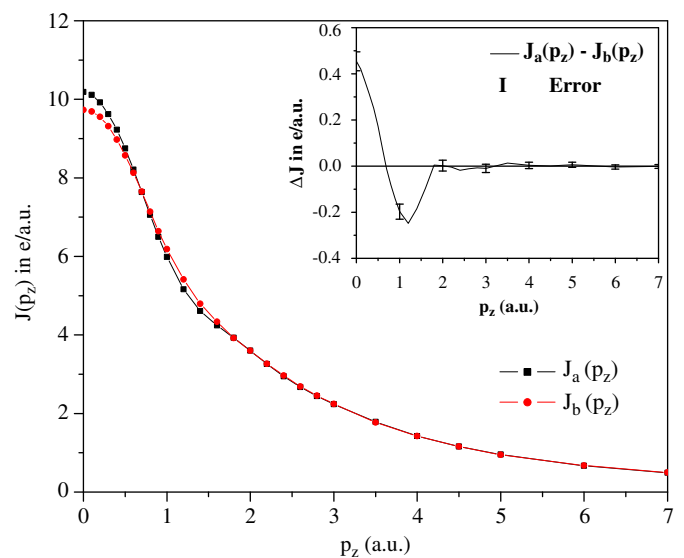


Fig. 4. Comparison of the earlier $[J_a(p_z)]$ and present $[J_b(p_z)]$ Compton profiles of bulk ZnS. The difference between the two measurements ($\Delta J = [J_a(p_z)] - [J_b(p_z)]$) is also presented in the inset. Experimental errors ($\pm \sigma$) are also shown at few points.

In Fig. 5, the experimental valence Compton profiles of ZnS nanomaterials and our new measurement on bulk sample are presented. The free atom profile given here is convoluted with the instrumental resolution function (Gaussian of FWHM 0.6 a.u.). The differences between profiles of nano-A and nano-B with respect to bulk ZnS, which primarily represents the differences in valence electron distribution are shown in the inset. From this figure, it can be seen that the Compton profile for valence electrons in free atom is the sharpest. The line width increases with the size of the nanoparticles. Since the Compton profiles of both the nano-sized samples are sharper than the bulk ZnS, it indicates the difference in the distribution of valence electron densities in these samples. The observed narrowness of Compton profiles can be interpreted due to the differences in density of valence electrons due to solid state effects, which are smaller in nanoparticles [30–32]. This also explains that when size of nanocrystals increases, the broadening of Compton profile also increases and approaches towards the broad profile due to bulk.

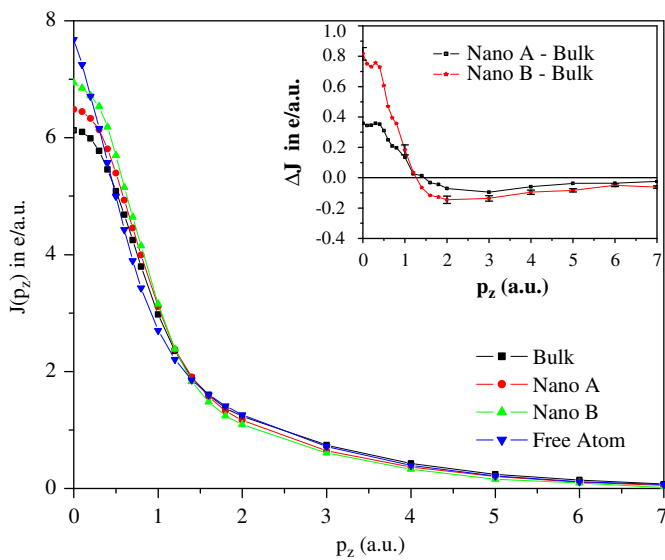


Fig. 5. Experimental valence Compton profiles of bulk and nano-phases of ZnS. The inset shows the differences between nano-A and nano-B to bulk ZnS.

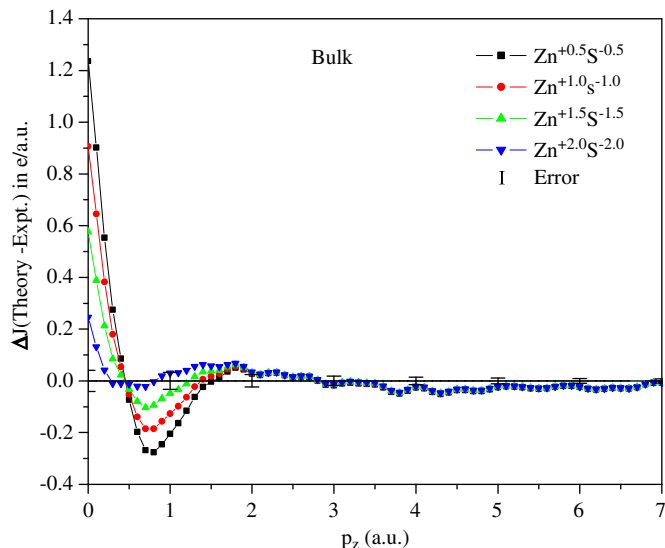


Fig. 6. Difference between convoluted ionic Compton profiles and the experimental Compton profile of bulk ZnS. Experimental errors ($\pm \sigma$) are also shown at a few points. All ionic profiles are convoluted with the Gaussian of 0.6 a.u. FWHM.

The theoretical Compton profiles of ZnS with varying ionic arrangements were calculated from the free atom profiles of Zn and S as taken from Biggs et al. [25]. The valence profiles for various $\text{Zn}^{+x}\text{S}^{-x}$ ($0.0 \leq x \leq 2$ in step of 0.5) configurations were calculated by transferring x electrons from 4s shell of zinc to the 3p shell of sulfur and the valence profiles for $\text{Zn}^{+x}\text{S}^{-x}$ were added to core contributions to get the total profiles. The difference profiles (convoluted theory—experiment) for various $\text{Zn}^{+x}\text{S}^{-x}$ (where x varies from 0 to 2 in a step of 0.5) configurations have been plotted in Figs. 6–8 for bulk, nano-A and nano-B samples respectively. From Figs. 6 to 8, it is evident that the effect of varying charge on Zn and S is visible in the region 0–2.0 a.u. and all configurations show identical nature for $p_z \geq 2.0$ a.u. On the basis of χ^2 test and also Figs. 6–8, it is obvious that configurations corresponding to $x=2.0, 1.8$ and 1.2 electrons give the best agreement with the experiment for bulk, nano-A and nano-B samples, respectively. Hence the ionic model suggests the transfer of 2.0, 1.8 and 1.2 electrons from the valence 4s state of Zn to the

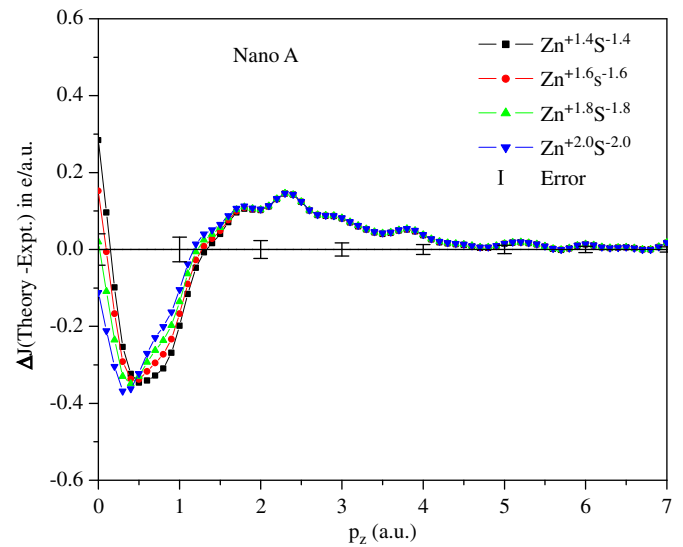


Fig. 7. Difference between convoluted ionic Compton profiles and the experimental Compton profile of nano-A. Experimental errors ($\pm \sigma$) are also shown at a few points. All ionic profiles are convoluted with the Gaussian of 0.6 a.u. FWHM.

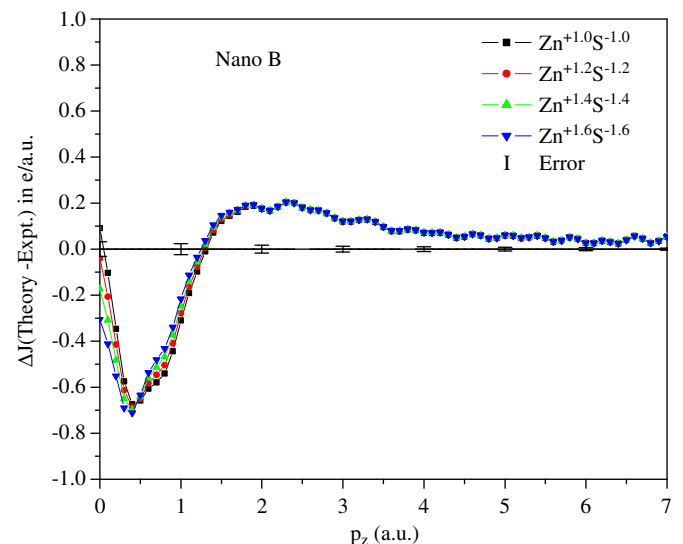


Fig. 8. Difference between convoluted ionic Compton profiles and the experimental Compton profile of nano-B. Experimental errors ($\pm \sigma$) are also shown at a few points. All ionic profiles are convoluted with the Gaussian of 0.6 a.u. FWHM.

3p state of S in bulk, nano-A and nano-B samples, respectively. Thus, the decreases in the charge transfer values on reduction of particle size indicate weak ionic bonding in smaller size particle of ZnS. There are no theoretical calculations reported on nano-sized ZnS samples, which would have enabled direct comparison with our data. It is hoped that the present work would stimulate further work along these lines from which accurate theoretical Compton profile of ZnS nanomaterials can be computed.

4. Conclusions

The isotropic Compton profile of ZnS nanoparticles are presented and compared with the measured profile of bulk and free atom Compton profile of ZnS. The experimental results indicate that there is significant change in valence electron distribution as we move from free atom to nano and then bulk sample. The ionic model suggests different amounts of charge transfer, which increases with the size, namely 1.2 and 1.8 electrons for nano-B and nano-A samples, respectively, which are smaller than the value 2.0 electrons for bulk ZnS. For a more meaningful comparison, accurate theoretical calculations on nano-sized ZnS and measurement of Compton profiles at high resolution are desirable.

Acknowledgements

This work is financially supported by the University Grant Commission (UGC) through Emeritus Fellowship and SR/33-37/2007 to BKS and SR/39-982/2010 to GS. The financial support provided by DST, New Delhi is also acknowledged.

References

[1] W.Q. Peng, G.W. Cong, S.C. Qu, Z.G. Wang, *Opt. Mater.* 29 (2006) 313.

- [2] C. Bouvy, F. Piret, W. Marine, B.L. Su, *Chem. Phys. Lett.* 433 (2007) 350.
 [3] R. Rossetti, J.L. Ellison, J.M. Gibson, L.E. Brus, *J. Chem. Phys.* 80 (1984) 4464.
 [4] K. Durose, P.R. Edwards, D.P. Halliday, *J. Cryst. Growth* 197 (1999) 733.
 [5] A.J. Hoffman, G. Mills, M.R. Hoffman, *J. Phys. Chem.* 96 (1992) 5546.
 [6] M.A. Hasse, J. Qui, J.M. De Puydt, H. Cheng, *Appl. Phys. Lett.* 59 (1991) 1272.
 [7] H. Kinto, M. Yagi, K. Tanigashira, T. Yamada, H. Uchiki, S.J. Iida, *Cryst. Growth* 117 (1992) 348.
 [8] G.D. Lee, M.H. Lee, J. Ihm, *Phys. Rev. B* 52 (1995) 1459.
 [9] C. Falcony, M. Garcia, A. Ortiz, J.C. Alonso, *J. Appl. Phys.* 72 (1992) 1525.
 [10] W. Tang, D.C. Cameron, *Thin Solid Films* 280 (1996) 221.
 [11] A.D. Yoffe, *Adv. Phys.* 42 (1993) 173.
 [12] X. Fang, T. Zhai, Ujjal K. Gautam, Liang Li, L. Wua, Y. Bando, D. Golberg, *Prog. Mater. Sci.* 56 (2011) 175.
 [13] N.R. Pawaskar, S.D. Sathaye, M.M. Bhadhade, K.R. Patil, *Mater. Res. Bull.* 37 (2002) 539.
 [14] Z. Nourbakhsh, *J. Alloys Compd.* 505 (2010) 698.
 [15] S.K. Gupta, S. Kumar, S. Auluck, *Opt. Commun.* 284 (2011) 20.
 [16] R. Saravanan, S. Saravanakumar, S. Lavanya, *Physica B* 405 (2010) 3700.
 [17] S.S. Nath, D. Chakdar, G. Gope, D.K. Avathi, *J. Nanotechnol.*, doi:10.2440/azojono0128.
 [18] X. Zhang, M. Zhao, T. He, W. Li, X. Lin, Z. Wang, Z. Xi, X. Liu, Y. Xia, *Solid State Commun.* 147 (2008) 165.
 [19] X. Zhang, H. Zhang, T. He, M. Zhao, *J. Appl. Phys.* 108 (2010) 64317.
 [20] M. Navaneethan, J. Archana, K.D. Nisha, Y. Hayakawa, S. Ponnusamy, C. Muthamizhchelvan, *J. Alloys Compd.* 506 (2010) 249.
 [21] Y. Pan, Jie Yu, Zhan Hu, H. Li, Q. Cu, G. Zou, *J. Mater. Sci. Technol.* 23 (2007) 193.
 [22] M.J. Cooper, *Rep. Prog. Phys.* 48 (1985) 415.
 [23] B. Williams, *Compton Scattering*, McGraw-Hill, New York, 1977; M.J. Cooper, P.E. Mijnarends, N. Shiotani, N. Sakai, A. Bansil, *X-ray Compton Scattering* Oxford University Press, 2004.
 [24] B.K. Panda, H.C. Padhi, *Phys. Status Solidi B* 166 (1991) 519.
 [25] F. Biggs, L.B. Mandelsohn, J.B. Mann, *At. Data Nucl. Data Tables* 16 (1975) 201.
 [26] B.K. Sharma, A. Gupta, H. Singh, S. Perkki, A. Kshirsagar, D.G. Kanhere, *Phys. Rev. B* 37 (1988) 6821.
 [27] D.N. Timms, Ph.D. Thesis University of Warwick, UK, unpublished, 1989.
 [28] J. Felsteiner, P. Pattison, M.J. Cooper, *Philos. Mag.* 30 (1974) 537.
 [29] A. Guinier, *X-ray Diffraction*, Freeman, San Francisco, 1963.
 [30] E.D. Isaacs, P. Platzman, *Phys. Today* 49 (1996) 40.
 [31] C. Metz, Th. Tschentscher, P. Suortti, A.S. Kheifets, D.R. Lun, T. Sattler, J.R. Schneider, F. Bell, *J. Phys.: Condens. Matter* 11 (1999) 3933.
 [32] G. Sharma, K.B. Joshi, M.C. Mishra, S. Shrivastava, Y.K. Vijay, B.K. Sharma, *Physica E* 43 (2011) 1084.